Checkerboards, stripes, and corner energies in spin models with competing interactions

Alessandro Giuliani

Dipartimento di Matematica, Università di Roma Tre, L.go S. L. Murialdo 1, IT-00146 Roma, Italy

Joel L. Lebowitz

Departments of Mathematics and Physics, Rutgers University, Piscataway, New Jersey 08854, USA

Elliott H. Lieb

Departments of Physics and Mathematics, Princeton University, P.O. Box 708, Princeton, New Jersey 08542, USA

We study the zero-temperature phase diagram of Ising spin systems in two dimensions in the presence of competing interactions: long-range antiferromagnetic and nearest-neighbor ferromagnetic of strength J. We first introduce the notion of a "corner energy," which shows, when the antiferromagnetic interaction decays faster than the fourth power of the distance, that a striped state is favored with respect to a checkerboard state when J is close to J_c, the transition to the ferromagnetic state, i.e., when the length scales of the uniformly magnetized domains become large. Next, we perform detailed analytic computations on the energies of the striped and checkerboard states in the cases of antiferromagnetic interactions with exponential decay and with power-law decay r^{-p}, $p > 2$, which depend on the Manhattan distance instead of the Euclidean distance. We prove that the striped phase is always favored compared to the checkerboard phase when the scale of the ground-state structure is very large. This happens for $J \lesssim J_c$ if $p > 3$, and for J sufficiently large if $2 < p \leqslant 3$. Many of our considerations involving rigorous bounds carry over to dimensions greater than two and to more general short-range ferromagnetic interactions.

PACS number(s): 75.10.−b, 75.70.−i, 05.50.+q

I. INTRODUCTION

In this paper, we continue our study of the ground state (GS) of lattice spin systems with competing ferromagnetic (F) and antiferromagnetic (AF) Ising-type spin interactions. See Refs. [1]–[4] for previous results. Such systems are simplified models of real systems with both short-range attractive interactions and long-range dipolar-type interactions. The competitive nature of these interactions is believed to be responsible for the formation of mesoscopic periodic structures, such as stripes, in many quasi-two-dimensional (2D) systems at low temperature (see Refs. [5]–[15] for several examples of spontaneous pattern formation in physical systems with competing interactions). See, also, Refs. [16] and [17] where such competition is held responsible for the development of macroscopic patterns in chemical and biological systems described by reaction-diffusion equations.

While it is simple to understand that the competition between interactions acting on different length scales can give rise to mesoscopic structures, it is very difficult to predict the optimal shape of these structures. The problem of determining the optimal shape and mutual arrangement of these domains has been addressed in the past by a variety of numerical and theoretical techniques, ranging from Monte Carlo simulations,[18]–[20] variational computations and energy estimates,[21]–[26] functional analytic estimates,[27,28] mean-field theory and self-consistent equations,[29]–[32] effective field theory, thermodynamic stability and local density approximation,[33]–[36] scaling arguments,[37] and renormalization group.[38,39] Similar methods have been used to predict the shape and size dependence of these structures on experimental parameters such as temperature[40]–[42] or, in the context of thin magnetic

films, the sample thickness,[26,43] the out-of-plane uniaxial anisotropy,[44] or an external magnetic field.[45,46] However, a fundamental understanding of the microscopic mechanism leading to a self-organized periodic pattern is still missing. Even at a heuristic or numerical level, the preferred pattern is often very difficult to identify due to the proliferation of quasidegenerate states and the slow glassylike approach to equilibrium.[47]–[51]

Here, we show for a large class of interactions that stripes are energetically favorable as compared to other natural structures, such as the rectangular or square checkerboard, by a combination of variational estimates, rigorous upper and lower bounds, and by analytical comparison of the energies of different patterns. The Hamiltonians we consider have the form

$$H = \frac{1}{2} \sum_{\mathbf{x} \neq \mathbf{y}} [-J \, \delta_{|\mathbf{x}-\mathbf{y}|,1} + \varepsilon \, v(\mathbf{x} - \mathbf{y})](\sigma_{\mathbf{x}}\sigma_{\mathbf{y}} - 1)$$

$$\equiv \frac{1}{2} \sum_{\mathbf{x} \neq \mathbf{y}} \phi(\mathbf{x} - \mathbf{y})(\sigma_{\mathbf{x}}\sigma_{\mathbf{y}} - 1) \,, \tag{1}$$

where $\mathbf{x} \in \mathbb{Z}^d$, $\sigma_{\mathbf{x}} = \pm 1$ are Ising spins, J and ε are two positive constants (the strengths of the F and AF interactions), v is a non-negative potential, symmetric with respect to $90°$ rotations and summable. In the following, we will be mostly concerned with $d = 2$ and v of infinite range. The constants J and ε will be thought of as being "large" and "small," respectively.

The goal is to understand the zero-temperature phase diagram as the ratio J/ε is varied. If $\varepsilon = 0$, the ground state is ferromagnetic. In the opposite limit, that is, $J = 0$, the ground

state displays some nontrivial alternation between positively and negatively magnetized domains; e.g., if $v(\mathbf{x}) = |\mathbf{x}|^{-p}$, $p > d$, then the ground state is the period-2 antiferromagnetic Néel state.[52] As the ratio J/ε is increased from zero to large values, the GS changes to reduce the number of antiferromagnetic bonds. This can be achieved by generating uniformly magnetized structures of larger and larger length scales. It is often assumed that the ground-state configurations are periodic, and display either checkerboard or striped order, depending on the specific choice of the interaction and the value of J. In Ref. 24, it was shown that, for $v(\mathbf{x}) = |\mathbf{x}|^{-3}$ and J large enough, the optimal striped configuration has lower energy than the optimal checkerboard configuration (contrary to the erroneous conclusions of Ref. 21, where a similar computation was performed). This leads to the conjecture [still unproven, but supported by several numerical works (see, e.g., Refs. 20,22, and 23)] that the ground-state configurations of Eq. (1) with $v(\mathbf{x}) = |\mathbf{x}|^{-3}$ and J large display periodic striped order.

There is also evidence for the fact that the sequence of transitions to the ferromagnetic phase has some universal features,[8,53–56] and that the emergence of stripes is essentially *independent of many details of the F and AF interactions*. However, the reason for this is still unclear and puzzling because stripes break the symmetry of the lattice.

In this paper, we prove that striped patterns are favored, within a natural class of variational states, when the scale of the GS structure is very large compared to the range of the FM interaction. A simple explanation of this fact can be based on the concept of *corner energy*, which suggests that the intersection points among straight phase separation lines can be thought of as elementary excitations of the system with positive energy, at least in the case that the AF interaction decays faster then r^{-4} at large distances. Our argument is substantiated by explicit computations in the simple case that the AF interaction depends on the Manhattan (L^1) distance between sites and decays as r^{-p}, $p > 2$, at large distances.

The rest of the paper is organized as follows. In Sec. II, we introduce the notions of line and corner energies and present our argument explaining why stripes are favored as compared to checkerboard when the AF interaction decays at infinity faster than r^{-4} and the scale becomes very large compared to the lattice spacing. In Sec. III, we present detailed analytical computations of the stripe and checkerboard energies in cases where the AF interaction depends on the Manhattan distance between sites and decays either exponentially or as a power law r^{-p}, $p > 2$. In Appendix A, we rigorously compute the critical strength J_c of the FM interaction separating a FM from a non-FM phase, when the AF interaction decays at infinity faster than r^{-3}. In Appendix B, we prove that power-law interactions depending on the Euclidean distance between sites are reflection positive. This implies that, if the GS consists of stripes, it will be periodic. Finally, in Appendix C, we discuss in some more detail the zero-temperature phase diagram of the model when the AF potential is an exponential Kac interaction; in this case, we have evidence for a transition from checkerboard to stripes as J is increased from zero to J_c. The conjecture is verified by rigorous upper and lower bounds on the GS energy.

II. LINES AND CORNERS

In this section, we show that the formation of stripes of mesoscopic size in $d = 2$ is essentially independent of the nature of the AF interaction in Eq. (1), as long as it is long range and falls off faster than $|\mathbf{x}|^{-4}$, i.e., $0 \leqslant v(\mathbf{x}) \leqslant K|\mathbf{x}|^{-4-\delta}$ for some constants $K, \delta > 0$. According to this argument, the occurrence of stripes is related to the sign and the relative sizes of line and corner energies, which we now define.

Consider a system in a square box of side length L with half the spins up and half down, separated by a vertical line, called an antiphase boundary. When the falloff of v is faster than $|\mathbf{x}|^{-3}$, the energy divided by L will have a nice limit as $L \to \infty$, which is defined to be the **line energy** τ:

$$\tau = -2 \lim_{L \to \infty} L^{-1} \sum_{\substack{-L/2 < x_1 \leqslant 0 \\ 1 \leqslant x_2 \leqslant L}} \sum_{\substack{1 \leqslant y_1 \leqslant L/2 \\ 1 \leqslant y_2 \leqslant L}} \phi(\mathbf{x} - \mathbf{y}). \quad (2)$$

The energy per unit length τ has the interpretation of *surface tension* of an infinite straight line, and is linear in J, i.e., $\tau = 2(J - J_c)$ for a suitable positive constant J_c.

At $J = J_c$, the surface tension of an infinite straight line vanishes and there is coexistence of the FM ground state with the ground state corresponding to a single isolated antiphase boundary. It is intuitive that, for all $J > J_c$, the ground state is ferromagnetic, since the energies of ferromagnetic contours (or, at least, of *straight* FM contours) are positive. See Appendix A for a proof of stability of the FM state against arbitrary contours. For $J < J_c$, the GS is certainly not FM, because the system reduces its energy by producing antiphase boundaries.

Next, we define a **corner energy** κ by first taking two crossed, vertical and horizontal, antiphase boundaries in the box of size L. The energy of this configuration is, to first approximation, $2\tau L$. The difference between this energy and $2\tau L$ has a limit as $L \to \infty$ whenever the falloff of v is faster than $|\mathbf{x}|^{-4}$. This difference is the corner energy κ, and is given by the formula

$$\kappa = 4 \sum_{\mathbf{x} \in Q_1} \sum_{\mathbf{y} \in Q_3} \phi(\mathbf{x} - \mathbf{y}) + 4 \sum_{\mathbf{x} \in Q_2} \sum_{\mathbf{y} \in Q_4} \phi(\mathbf{x} - \mathbf{y}), \quad (3)$$

where Q_1, Q_2, Q_3, and Q_4 are the first, second, third, and fourth quadrant in $\mathbb{Z}^2$, respectively. Note that κ does not depend on the nearest-neighbor interaction energy and is therefore positive for the Hamiltonian in Eq. (1).

We now observe that, if the GS is made up of a rectangular checkerboard (not necessarily periodic), then it consists of a mixture of horizontal and vertical lines, and hence has corners where these lines intersect. To lower the energy, one can replace the horizontal lines by the same number of vertical lines, thereby eliminating the corners. While the increased density of vertical lines increases the energy, the saving on the corners more than makes up for it when the scale is large enough and $J \lesssim J_c$. In fact, consider a configuration of sparse straight lines, all typically at a mutual distance larger than $R \gg 1$. The interaction energy of any vertical (resp. horizontal) line in a square box of side L with all the other vertical (resp. horizontal) lines is positive and smaller than (const) $L R^{-1-\delta}$, which follows from the fact that $0 \leqslant v(\mathbf{x}) \leqslant K|\mathbf{x}|^{-4-\delta}$. Similarly, the

interaction energy of any corner with all the other corners is negative and smaller in absolute value than (const) $R^{-\delta}$. Therefore, the total energy E_Λ of a configuration of widely separated straight lines in a square box $\Lambda \subset \mathbb{Z}^2$ of side L has the form

$$E_\Lambda = [\tau + O(R^{-1-\delta})](M_1 + M_2)L + [\kappa - O(R^{-\delta})]\, M_1 M_2, \tag{4}$$

where M_1 (M_2) is the total number of horizontal (vertical) lines and we recall that the line energy $\tau = 2(J - J_c)$ is *negative* for the considered values of J, $J \lesssim J_c$. Equation (4) shows that, for given $M = M_1 + M_2$ of order L/R, it is energetically favorable to have $M_1 M_2 \ll L^2/R^2$. In fact, if the number of corners was $\simeq L^2/R^2$, than we could decrease the energy by rotating all the vertical (horizontal) lines by $90°$, making them horizontal (vertical) and placing them halfway between the existing horizontal (vertical) lines. The decrease in energy due to elimination of the corners would be of the order L^2/R^2, while the increase, due to increased repulsion energy between lines, would be of the order $L^2/R^{2+\delta}$, which is much smaller. Therefore, after this rotation, the final configuration would have an energy equal to $[-|\tau| + O(R^{-1-\delta})](M_1 + M_2)L$, which is strictly smaller than the one of the initial configuration. From this expression, it is apparent that the optimal line separation, which can be computed by balancing the line energy with the repulsion energy between lines, is of the order $R \simeq |\tau|^{1/(1+\delta)}$. Therefore, having R large requires having $|\tau|$ small, that is, J sufficiently close to the critical value J_c. This also indicates that the GS energy per site scales as $-|\tau|^{(2+\delta)/(1+\delta)}$ at small negative values of τ. By the methods of Appendix A, we can prove a rigorous lower bound, showing that the actual GS energy scales exactly as $-|\tau|^{(2+\delta)/(1+\delta)}$ for τ small and negative. This is a strong indication for stripes in the parameter range under consideration.

The previous discussion shows that *corners play the role of elementary excitations, with a positive energy cost, which can be eliminated by rotating straight lines by $90°$.* A similar analysis shows that also the "half corners" produced each time that a nonstraight antiphase boundary has a $90°$ turn have a finite positive cost. Therefore, we can give a similar argument to exclude the presence of large isolated rectangles in the GS. We are, however, not able to exclude the presence of more complicated "excitations" in the GS.

Regarding the condition on the large distance decay of the AF interactions, we do not think it is sharp. However, in the general case, the balance between the corner and line energies is much more subtle. In fact, if the decay of the AF potential is $\sim r^{-p}$, $2 < p < 4$, then the corner energy is formally infinite; however, corner-corner interactions have an oscillatory sign and such oscillations make the effective energy of each corner finite and approximately proportional to R^{4-p} if $2 < p < 4$, where R is the distance to the neighboring corner. It is straightforward to check that, if the corners have a finite density, then their contribution to the specific GS energy is comparable to the line-line interaction and of the order of R^{2-p}, where R is the typical separation between lines. Therefore, by rotating the vertical lines by $90°$, we gain the corner energies and lose some line-line interaction energy, both of the order (const)$R^{2-p}L^2$; to decide whether the saving makes up for the loss, we need to compute the

constant prefactors. This will be done analytically in the next section, in the special case of AF interactions depending on the Manhattan distance between sites. The computation shows that, when we rotate the vertical lines by $90°$ and eliminate the corners, the saving overcomes the loss for all $p > 2$. It remains to be seen whether this saving is an accident of the specific model considered below or whether there is a general physical reason behind the result.

We note that in the special case that the AF interaction is reflection positive,[52] given that the configurations entering the GS are all straight vertical (horizontal) lines, then they have to be periodically arranged. This follows from the analysis in Refs. 1–4.

III. COMPARISON OF THE STRIPE AND CHECKERBOARD ENERGIES

In this section, we perform explicit analytic computations of the energies of the stripe and checkerboard states for different choices of the falloff of the long-range AF potential. We focus on the (analytically) simple case of interactions depending on the Manhattan (L_1) distance $\|\mathbf{x}\|_1 := |x_1| + |x_2|$ between sites. Our calculations complement and simplify those in Ref. 24.

Let us consider Eq. (1) with $d = 2$, $\varepsilon = 1$, and

$$v(\mathbf{x}) = \int_0^\infty d\alpha \, \mu(\alpha) e^{-\alpha \|\mathbf{x}\|_1} \,, \tag{5}$$

with $\mu(\alpha)$ a positive measure. We will be particularly concerned with two cases:

(i) exponential interactions $v(\mathbf{x}) = \gamma^2 e^{-\gamma \|\mathbf{x}\|_1}$ corresponding to the choice $\mu(\alpha) = \gamma^2 \delta(\alpha - \gamma)$ in Eq. (5);

(ii) power-law interactions $v(\mathbf{x}) = \|\mathbf{x}\|_1^{-p}$, with $p > 2$, corresponding to the choice $\mu(\alpha) = \alpha^{p-1}/\Gamma(p)$ in Eq. (5).

As mentioned above, the choice Eq. (5) is made to simplify the computations; choosing Euclidean rather than Manhattan distance should not make a difference from the physical point of view. Let us remark that the potential in Eq. (5) is *reflection positive*[52] and so is the (more usual) power-law potential $v(\mathbf{x}) = |\mathbf{x}|^{-p}$, with $|\mathbf{x}| = \sqrt{x_1^2 + x_2^2}$ the Euclidean distance (see Appendix B). The property of reflection positivity is not explicitly used in the computations below but, as observed at the end of previous section, it implies that if the GS consists of stripes, then these must be regularly spaced (see Refs. 1–4).

Let $s_h(x)$ be the one-dimensional (1D) profile of period $2h$, obtained by extending periodically over $\mathbb{Z}$ the function $f : (-h,h] \rightarrow \mathbb{R}$ such that $f(x) = \mathrm{sign}(x - 1/2)$ for $x = -h + 1, \ldots, h$. Let $e_c(h)$ be the specific energy of the checkerboard configuration $\sigma_{\mathbf{x}} = s_h(x_1)s_h(x_2)$, and let $e_s(h)$ be the specific energy of the striped configuration $\sigma_{\mathbf{x}} = s_h(x_1)$. We start by computing the specific energy $e(h_1,h_2)$ of the "rectangular" configuration $s_{h_1}(x_1)s_{h_2}(x_2)$. We have

$$
\begin{aligned}
e(h_1,h_2) = {} & \frac{2J}{h_1} + \frac{2J}{h_2} - \frac{1}{h_1 h_2} \int_0^\infty d\alpha \mu(\alpha) \\
& \times \sum_{\substack{1 \leqslant x_1 \leqslant h_1 \\ 1 \leqslant x_2 \leqslant h_2}} \sum_{\mathbf{y} \in \mathbb{Z}^2} e^{-\alpha|x_1 - y_1|} e^{-\alpha|x_2 - y_2|} \chi(\sigma_{\mathbf{x}} \neq \sigma_{\mathbf{y}}),
\end{aligned}
$$

$$\tag{6}$$

where χ(condition) is $= 1$ if the condition is satisfied and $= 0$ otherwise. After some straightforward algebra,

$$e(h_1,h_2) = \frac{2J}{h_1} + \frac{2J}{h_2} + 2 \int_0^\infty \frac{d\alpha}{\alpha^2} \, \mu(\alpha) \left[-A_\alpha \frac{\tanh(\alpha h_1/2)}{\alpha h_1/2} \right.$$
$$\left. -A_\alpha \frac{\tanh(\alpha h_2/2)}{\alpha h_2/2} + B_\alpha \frac{\tanh(\alpha h_1/2)}{\alpha h_1/2} \frac{\tanh(\alpha h_2/2)}{\alpha h_2/2} \right], \tag{7}$$

where

$$A_\alpha = \frac{(\alpha/2)^3 \cosh(\alpha/2)}{\sinh^3(\alpha/2)} , \qquad B_\alpha = \frac{(\alpha/2)^4}{\sinh^4(\alpha/2)} . \tag{8}$$

Note that, for small α, $A_\alpha \simeq 1 - (1/15)(\alpha/2)^4$ and $B_\alpha \simeq 1 - (2/3)(\alpha/2)^2$, which will be useful in the following.

Using Eq. (7), we see that the energy of a striped configuration of period h is equal to

$$e_s(h/2) = \frac{4J}{h} + 2 \int_0^\infty \frac{d\alpha}{\alpha^2} \, \mu(\alpha) \left[-2A_\alpha \frac{\tanh(\alpha h/4)}{\alpha h/2} \right], \tag{9}$$

while the one of a checkerboard configuration of period $2h$ is

$$e_c(h) = \frac{4J}{h} + 2 \int_0^\infty \frac{d\alpha}{\alpha^2} \, \mu(\alpha) \left[-2A_\alpha \frac{\tanh(\alpha h/2)}{\alpha h/2} \right.$$
$$\left. +B_\alpha \frac{\tanh^2(\alpha h/2)}{(\alpha h/2)^2} \right]. \tag{10}$$

It is interesting to note that the various terms in Eqs. (7), (9), and (10) have a clear interpretation in terms of the notions of "line energy" and "corner energy," introduced in Sec. II. In fact, looking at Eq. (7), the terms proportional to J correspond to the FM surface tension energy; the integral terms with the integrand proportional to A_α correspond to the AF line energy (including both the negative AF surface tension and the repulsive line-line interactions); the integral term with the integrand proportional to B_α corresponds to the AF corner energy (including both the positive corner self-energy and the attractive corner-corner interactions). The analogous terms in Eqs. (9) and (10) have a similar interpretation; note that $e_c(h)$ includes a positive contribution from the corner energy, which does not appear in $e_s(h/2)$, while the contribution from the line energy is smaller than the corresponding one in $e_s(h/2)$.

As we discussed above, the goal is to find the balance between these terms when the scale of the relevant structures is large compared to the lattice spacing. We will, in fact, show that when $h \gg 1$, then $e_c(h) > e_s(h/2)$, which is equivalent to

$$\frac{1}{2} \int_0^\infty \frac{d\alpha}{\alpha^2} \, \mu(\alpha) \, B_\alpha \frac{\tanh^2(\alpha h/2)}{(\alpha h/2)^2}$$
$$> \int_0^\infty \frac{d\alpha}{\alpha^2} \, \mu(\alpha) \, A_\alpha \frac{\tanh(\alpha h/2) - \tanh(\alpha h/4)}{\alpha h/2}, \tag{11}$$

implying that the GS is striped. This will be proved below by treating separately the cases of exponential interactions and of power-law interactions, with $p > 4$, $p = 4$, $3 < p < 4$, $p = 3$, $2 < p < 3$ (which are listed here in the order of increasing difficulty).

Remark. Even though Eq. (11) does not involve the parameter J, the condition that the scale h of the GS structures is large compared to the lattice spacing is satisfied only if J is chosen properly. More precisely, as discussed in Sec. II (see also Appendix A), if the AF interaction decays faster than r^{-3}, then there exists a finite J_c such that the homogeneous FM state is the GS for all $J \geqslant J_c$; in this case, the condition that $h \gg 1$ is valid in the range $J \lesssim J_c$. On the contrary, if the decay of the AF interaction is equal to r^{-3} or slower, then the condition $h \gg 1$ is verified for all $J \gg 1$. The results below are relevant for J belonging to these ranges.

A. Exponential interactions and power laws with $p > 4$

If the AF interaction decays exponentially or as a power law with $p > 4$, then we already know from the analysis in Sec. II that $e_c(h) > e_s(h/2)$ for all $h \gg 1$. For completeness, let us check this analytically, using Eq. (11). In the case of exponential interactions, the condition reduces to

$$\frac{1}{2} B_\gamma \frac{\tanh^2(\gamma h/2)}{(\gamma h/2)^2} > A_\gamma \frac{\tanh(\gamma h/2) - \tanh(\gamma h/4)}{\gamma h/2}, \tag{12}$$

which is obviously satisfied for h large, simply because the left-hand side goes to zero as h^{-2}, while the right-hand side goes to zero exponentially fast in h. In the case of power-law interactions with $p > 4$, the left-hand side of Eq. (11) can be rewritten as

$$\frac{1}{2} \int_0^\infty d\alpha \, \alpha^{p-3} \, B_\alpha \frac{\tanh^2(\alpha h/2)}{(\alpha h/2)^2}$$
$$= \frac{2}{h^2} \int_0^\infty d\alpha \, \alpha^{p-5} B_\alpha \left(\frac{1}{h^{p-2}} \right), \tag{13}$$

while the right-hand side is

$$\int_0^\infty d\alpha \, \alpha^{p-3} \, A_\alpha \frac{\tanh(\alpha h/2) - \tanh(\alpha h/4)}{\alpha h/2}$$
$$= \frac{1}{h^{p-2}} \int_0^\infty d\alpha \, \alpha^{p-3} \frac{\tanh(\alpha/2) - \tanh(\alpha/4)}{\alpha/2} + O\left(\frac{1}{h^{p+2}} \right), \tag{14}$$

where, in estimating the error term of order h^{-p-2}, we used the fact that $|A_\alpha - 1| \leqslant C\alpha^4$ for a suitable constant C. Therefore, Eq. (11) is valid, simply because $h^{-2} \gg h^{-p+2}$, $\forall p > 4$ for h large.

B. The case $p = 4$

This case is very similar to the previous one. In fact, the right-hand side can be rewritten and estimated exactly as in Eq. (14), with $p = 4$; in particular, it is $\sim h^{-2}$. The left-hand side can be rewritten as

$$\frac{1}{2} \int_0^\infty d\alpha \, \alpha \, B_\alpha \frac{\tanh^2(\alpha h/2)}{(\alpha h/2)^2}$$
$$= \frac{2}{h^2} \int_{1/h}^1 \frac{d\alpha}{\alpha} \tanh^2(\alpha h/2) + O\left(\frac{1}{h^2} \right)$$
$$= 2 \frac{\log h}{h^2} + O\left(\frac{1}{h^2} \right). \tag{15}$$

Therefore, Eq. (11) is valid simply because $h^{-2}\log h \gg h^{-2}$ for h large.

C. The case $p < 4$

If $p < 4$, the proof of Eq. (11) is slightly more subtle because both sides of the inequality scale in the same way as $h \to \infty$. In fact, the left-hand side can be rewritten as

$$\frac{1}{2}\int_0^\infty d\alpha\, \alpha^{p-3} B_\alpha \frac{\tanh^2(\alpha h/2)}{(\alpha h/2)^2}$$
$$= \frac{1}{2}\left(\frac{2}{h}\right)^{p-2}\int_0^\infty d\alpha\, \alpha^{p-3}\frac{\tanh^2\alpha}{\alpha^2} + O\left(\frac{1}{h^2}\right), \quad (16)$$

while the right-hand side reads as

$$\int_0^\infty d\alpha\, \alpha^{p-3} A_\alpha \frac{\tanh(\alpha h/2)-\tanh(\alpha h/4)}{\alpha h/2}$$
$$= \left(\frac{2}{h}\right)^{p-2}\int_0^\infty d\alpha\, \alpha^{p-3}\frac{\tanh\alpha-\tanh(\alpha/2)}{\alpha}+O\left(\frac{1}{h^{p+2}}\right). \quad (17)$$

Therefore, both sides of Eq. (11) scale as $\sim h^{2-p}$ as $h \to \infty$. The inequality is asymptotically valid if and only if the following condition is true:

$$\frac{1}{2}\int_0^\infty d\alpha\, \alpha^{p-3}\frac{\tanh^2\alpha}{\alpha^2} > \int_0^\infty d\alpha\, \alpha^{p-3}\frac{\tanh\alpha-\tanh(\alpha/2)}{\alpha}. \quad (18)$$

This inequality can be checked numerically in the different ranges $3 < p < 4$, $p = 3$, and $2 < p < 3$. In fact, if $p = 3$, Eq. (18) is equivalent to

$$\frac{1}{2}\int_0^\infty d\alpha\, \frac{\tanh^2\alpha}{\alpha^2} = 0.852\,56\ldots > \log 2 = 0.693\,15\ldots. \quad (19)$$

If $3 < p < 4$, Eq. (18) is equivalent to

$$\frac{1}{2}\int_0^\infty d\alpha\, \alpha^{p-5}\tanh^2\alpha > (2^{p-3}-1)\int_0^\infty d\alpha\, \alpha^{p-4}(1-\tanh\alpha). \quad (20)$$

In the limiting case $p \to 3^+$, Eq. (20) is equivalent to Eq. (19), as it should. In the limit $p \to 4^-$, Eq. (20) is obviously valid (because the right-hand side tends to a constant, while the left-hand side diverges to $+\infty$). The validity of Eq. (20) for all values of p in the interval $(3,4)$ can be checked numerically (see Fig. 1).

Finally, if $2 < p < 3$, Eq. (18) is equivalent to

$$\frac{1}{2}\int_0^\infty d\alpha\, \alpha^{p-5}\tanh^2\alpha > (1-2^{p-3})\int_0^\infty d\alpha\, \alpha^{p-4}\tanh\alpha. \quad (21)$$

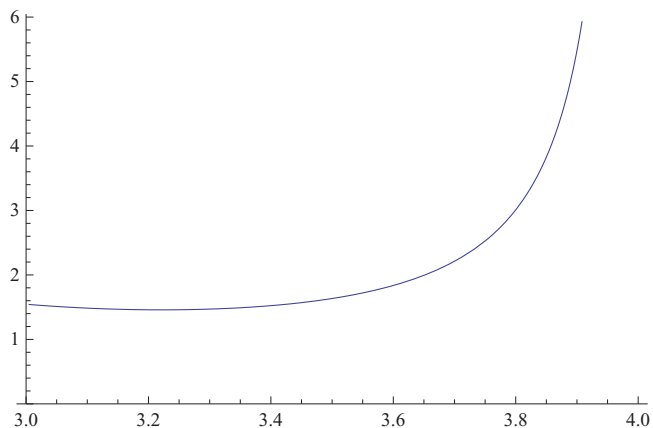FIG. 1. A plot of the difference between the right- and left-hand sides of (20) vs p, which proves that $e_s(h/2) < e_c(h)$ for all $3 < p < 4$, and h large enough.

In the limit $p \to 3^-$, condition (21) reduces to Eq. (19), as it should. In the limit $p \to 2^+$, condition (21) reduces to

$$\log 2 > \int_0^\infty d\alpha \left(\frac{\tanh\alpha}{\alpha^2} - \frac{\tanh^2\alpha}{\alpha^3}\right) \iff \log 2 + \frac{1}{2}$$
$$= 1.193\,147\ldots > \int_0^\infty d\alpha\, \frac{\tanh^3\alpha}{\alpha^2} = 1.154\,785\ldots. \quad (22)$$

The validity of Eq. (21) for all values of p in the interval $(2,3)$ can be checked numerically (see Fig. 2).

This concludes the proof that $e_c(h) > e_s(h/2)$, whenever h is large, for all power-law decays with exponent $p > 2$ and for exponential interactions. An immediate consequence of this analysis is the following: let $e_s^*(J) = \min_{h\in\mathbb{N}} e_s(h)$ and $e_c^*(J) = \min_{h\in\mathbb{N}} e_c(h)$ be the optimal stripe and checkerboard energies at a given J; then, if the AF interaction is either exponential or power law with $p > 3$, we have $e_s^*(J) < e_c^*(J)$ for all $J_c - J$ positive and small enough; if the AF interaction is power law with $2 < p \leqslant 3$, then $e_s^*(J) < e_c^*(J)$ for all J large enough.
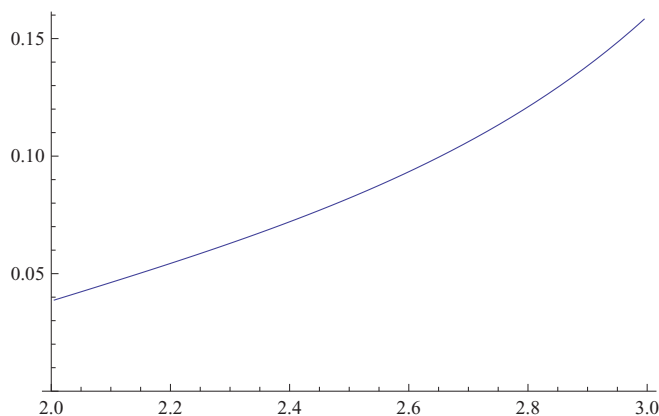

FIG. 2. A plot of the difference between the right- and left-hand sides of (21) vs p, which proves that $e_s(h/2) < e_c(h)$ for all $2 < p < 3$, and h large enough.

In conclusion, we showed for a two-dimensional spin model with competing short-range (nearest-neighbor) FM and long-range AF interactions that stripes are favored with respect to checkerboard when the GS structures are large compared to the range of the FM interaction. If the AF interaction decays faster than r^{-4}, the emergence of stripes close to the transition to the FM phase can be understood on the basis of a comparison between the sign and relative sizes of the corner and line energies, which is independent of the details of the AF interaction. If the decay at infinity of the AF interaction is slower, then the balance between corner and line energies is more subtle, and the understanding of why stripes are favored relies on explicit computations of the stripe and checkerboard energies, which have been performed here in the simple case that the AF depends on the Manhattan distance between sites. We believe that future progress on the problem will come from a deeper understanding of the reason that interactions that fall off slower than r^{-4} always seem to favor stripes.

ACKNOWLEDGMENTS

APPENDIX A: A RIGOROUS COMPUTATION OF J_c

Let us assume that the long-range AF interaction decays at infinity faster than r^{-3}, and let $\tau = 2(J - J_c)$ be the line energy, as defined in Sec. II. Here, we want to prove that, for all $J \geqslant J_c$, the homogeneous FM state is a GS of Eq. (1) (and is the unique GS for $J > J_c$). As already remarked in Sec. II, for $J < J_c$, the homogeneous state is *not* a GS, simply because the state with a single straight antiphase boundary has negative energy. If $J \geqslant J_c$, we want to get a lower bound on the energy of an arbitrary state, which is positive, unless the state is homogeneous.

We proceed in a way similar to the proof of Theorem 3 of Ref. 1. We need to introduce some definitions; in particular, via the basic Peierls construction, we introduce the definitions of *contours* and *droplets*. Given any spin configuration $\underline{\sigma}_\Lambda$ on the squared periodic box Λ, we define Δ to be the set of sites at which $\sigma_i = -1$, i.e., $\Delta = \{i \in \Lambda : \sigma_i = -1\}$. We draw around each $i \in \Delta$ the four sides of the unit square centered at i and suppress the sides that occur twice: we obtain in this way a *closed polygon* $\Gamma(\Delta)$, which can be thought as the boundary of Δ. Each side of $\Gamma(\Delta)$ separates a point $i \in \Delta$ from a point $j \notin \Delta$. At every vertex of $\Gamma(\Delta) \cap \Lambda^*$, with Λ^* the dual lattice of Λ, there can be either two or four sides meeting. In the case of four sides, we deform slightly the polygon, "chopping off" the edge from the squares containing a negative spin. When this is done, $\Gamma(\Delta)$ splits into disconnected polygons $\Gamma_1, \ldots, \Gamma_r$ which are called *contours*. Note that, because of the choice of periodic boundary conditions, all contours are closed but can possibly wind around the box Λ. The definition

of contours naturally induces a notion of connectedness for the spins in Δ: given $i, j \in \Delta$, we shall say that i and j are connected if there exists a sequence $(i = i_0, i_1, \ldots, i_n = j)$ such that i_m, i_{m+1}, $m = 0, \ldots, n-1$, are nearest neighbors and none of the bonds (i_m, i_{m+1}) crosses $\Gamma(\Delta)$. The maximal connected components δ_i of Δ will be called *droplets* and the set of droplets of Δ will be denoted by $\mathcal{D}(\Delta) = \{\delta_1, \ldots, \delta_s\}$. Note that the boundaries $\Gamma(\delta_i)$ of the droplets $\delta_i \in \mathcal{D}(\Delta)$ are all distinct subsets of $\Gamma(\Delta)$ with the property $\cup_{i=1}^s \Gamma(\delta_i) = \Gamma(\Delta)$.

Given the definitions above, let us rewrite the energy $E_\Lambda(\underline{\sigma}_\Lambda)$ of $\underline{\sigma}_\Lambda$ in a box $\Lambda \subset \mathbb{Z}^2$ with periodic boundary conditions as

$$E_\Lambda(\underline{\sigma}_\Lambda) = 2J \sum_{\Gamma \in \Gamma(\Delta)} |\Gamma| - \sum_{\delta \in \mathcal{D}(\Delta)} E_{\mathrm{dip}}(\delta), \qquad \text{(A1)}$$

where $E_{\mathrm{dip}}(\delta) := 2\varepsilon \sum_{\mathbf{x} \in \delta} \sum_{\mathbf{y} \in \Delta^c} v(\mathbf{x} - \mathbf{y})$, which can be bounded from above as

$$E_{\mathrm{dip}}(\delta) = 2\varepsilon \sum_{\mathbf{n} \in \mathbb{Z}^2} v(\mathbf{n}) \sum_{\mathbf{x} \in \delta} \sum_{\mathbf{y} \in \Delta^c} \chi(\mathbf{x} - \mathbf{y} = \mathbf{n})$$
$$\leqslant 2\varepsilon \sum_{\mathbf{n} \in \mathbb{Z}^2} v(\mathbf{n}) \sum_{\mathbf{x} \in \delta} \sum_{\mathbf{y} \in \mathbb{Z}^2 \setminus \delta} \chi(\mathbf{x} - \mathbf{y} = \mathbf{n}). \quad \text{(A2)}$$

Now, the number of ways in which $\mathbf{n} = (n_1, n_2)$ may occur as the difference $\mathbf{x} - \mathbf{y}$ or $\mathbf{y} - \mathbf{x}$ with $\mathbf{x} \in \delta$ and $\mathbf{y} \notin \delta$ is at most $\sum_{\Gamma \in \Gamma(\delta)} \sum_{i=1}^2 |\Gamma|_i |n_i|$, where $|\Gamma|_i$ is the number of faces in Γ orthogonal to the ith coordinate direction. Therefore,

$$E_{\mathrm{dip}}(\delta) \leqslant \varepsilon \sum_{\Gamma \in \Gamma(\delta)} \sum_{\mathbf{n} \in \mathbb{Z}^2} v(\mathbf{n}) \sum_{i=1}^2 |\Gamma|_i |n_i|$$
$$= 2\varepsilon \sum_{\Gamma \in \Gamma(\delta)} |\Gamma| \sum_{\substack{\mathbf{n} \in \mathbb{Z}^2: \\ n_1 > 0}} n_1 v(\mathbf{n}) = 2J_c \sum_{\Gamma \in \Gamma(\delta)} |\Gamma|.$$
$$\text{(A3)}$$

Plugging this back into Eq. (A1) gives

$$E_\Lambda(\underline{\sigma}_\Lambda) \geqslant 2(J - J_c) \sum_{\Gamma \in \Gamma(\Delta)} |\Gamma|, \qquad \text{(A4)}$$

which readily implies that the uniformly magnetized state is a GS for all $J \geqslant J_c$ and that it is the only GS for $J > J_c$.

As remarked in Sec. II [see the paragraph after Eq. (4)], the same method leading to Eq. (A4) allows us to prove that, as $\tau = 2(J - J_c)$ tends to zero from the left, the specific ground-state energy scales as $-|\tau|^{(2+\delta)/(1+\delta)}$, which is the same scaling as the optimal stripes energy for τ small and negative. However, we will not belabor the details of this computation here.

APPENDIX B: REFLECTION POSITIVITY OF POWER-LAW INTERACTIONS

In this appendix, we prove that $v(\mathbf{x}) = |\mathbf{x}|^{-p}$, with $p > 0$ and $|\mathbf{x}| \equiv |\mathbf{x}|_2 = \sqrt{x_1^2 + x_2^2}$ the usual Euclidean distance, is a reflection-positive (RP) potential, which may be a useful remark for a possible future proof of the periodicity of the GS

of Eq. (1) with $v(\mathbf{x}) = |\mathbf{x}|^{-p}$. We recall that v is RP if, for all compactly supported functions $f : \mathbb{Z}^2 \to \mathbb{C}$,

$$\sum_{\substack{x_1, y_1 \geqslant 1 \\ x_2, y_2 \in \mathbb{Z}}} \bar{f}_{\mathbf{x}} \, f_{\mathbf{y}} \, v(x_1 + y_1 - 1, x_2 - y_2) \geqslant 0. \qquad \text{(B1)}$$

By Schur's product theorem, pointwise products of RP potentials are reflection positive. Therefore, in order to prove that $|\mathbf{x}|^{-p}$ is RP for all $p > 0$, it is enough to show that $|\mathbf{x}|^{-1}$ and $|\mathbf{x}|^{-\lambda}$, with $0 < \lambda < 1$, are separately RP. If $v(\mathbf{x}) = |\mathbf{x}|^{-1}$ and $x_1 \geqslant 1$,

$$\begin{aligned} v(x_1, x_2) &= \frac{1}{\sqrt{x_1^2 + x_2^2}} \\ &= \frac{1}{2\pi^2} \int_{-\infty}^{+\infty} dk \int_{-\infty}^{+\infty} dp \int_{-\infty}^{+\infty} dq \, \frac{e^{ikx_1 + ipx_2}}{k^2 + p^2 + q^2} \\ &= \frac{1}{2\pi} \int_{-\infty}^{+\infty} dp \int_{-\infty}^{+\infty} dq \, \frac{e^{ipx_2}}{\sqrt{p^2 + q^2}} e^{-x_1\sqrt{p^2 + q^2}}, \end{aligned}$$
$$\text{(B2)}$$

from which (B1) readily follows. If $v(\mathbf{x}) = |\mathbf{x}|^{-\lambda}$, with $0 < \lambda < 1$, then (B1) follows if we prove the stronger result

$$\int_0^\infty dx_1 \int_{-\infty}^0 dy_1 \int_{-\infty}^{+\infty} dx_2 \int_{-\infty}^{+\infty} dy_2 \, \frac{\rho(\mathbf{x})\rho(\mathbf{y})}{|\mathbf{x} - \mathbf{y}|^\lambda} \geqslant 0, \quad \text{(B3)}$$

if $\rho(\mathbf{x})$ is a smooth compactly supported real function, with support contained in $\mathbb{R}^2 \setminus \{x_1 = 0\}$, and such that $\rho(-x_1, x_2) = \rho(x_1, x_2)$. Using the Fourier transform of $|\mathbf{x}|^{-\lambda}$ (see, e.g., Ref. 57, Theorem 5.9]), and proceeding as in Ref. 58, we can rewrite the left-hand side of (B3) as

$$\begin{aligned} &\frac{1}{2^\lambda \pi} \frac{\Gamma\left(1 - \frac{\lambda}{2}\right)}{\Gamma\left(\frac{\lambda}{2}\right)} \int_{\mathbb{R}^2} d\mathbf{k} \int_{\substack{x_1, y_1 > 0 \\ x_2, y_2 \in \mathbb{R}}} \\ &\times d\mathbf{x}\, d\mathbf{y}\, \rho(\mathbf{x}) \frac{e^{ik_1(x_1 + y_1)} e^{ik_2(x_2 - y_2)}}{\left(k_1^2 + k_2^2\right)^{1 - \lambda/2}} \rho(\mathbf{y}). \end{aligned} \qquad \text{(B4)}$$

We observe that, for fixed $x_1 + y_1 > 0$ and k_2, the function $e^{ik_1(x_1 + y_1)}(k_1^2 + k_2^2)^{-1 + \lambda/2}$ is analytic in k_1 in the upper half plane with the cut $\{i\tau : \tau \geqslant |k_2|\}$ removed. Deforming the contour of integration in dk_1 to this cut and calculating the jump of the argument across it, we obtain

$$\begin{aligned} &\int_{-\infty}^{+\infty} dk_1 \frac{e^{ik_1(x_1 + y_1)}}{\left(k_1^2 + k_2^2\right)^{1 - \lambda/2}} \\ &= 2\sin[\pi(1 - \lambda/2)] \int_{|k_2|}^\infty d\tau \frac{e^{-\tau(x_1 + y_1)}}{\left(\tau^2 - k_2^2\right)^{1 - \lambda/2}}. \end{aligned} \qquad \text{(B5)}$$

Plugging this back into (B4), we find

$$\begin{aligned} &\int_{\substack{-x_1, y_1 > 0 \\ x_2, y_2 \in \mathbb{R}}} \frac{\rho(\mathbf{x})\rho(\mathbf{y})}{|\mathbf{x} - \mathbf{y}|^\lambda} = \frac{2^{1-\lambda}}{\pi} \frac{\Gamma\left(1 - \frac{\lambda}{2}\right)}{\Gamma\left(\frac{\lambda}{2}\right)} \sin[\pi(1 - \lambda/2)] \\ &\times \int_{\mathbb{R}} dk_2 \int_{|k_2|}^\infty d\tau \frac{1}{\left(\tau^2 - k_2^2\right)^{1 - \lambda/2}} \int_{\substack{x_1, y_1 > 0 \\ x_2, y_2 \in \mathbb{R}}} \\ &\times d\mathbf{x}d\mathbf{y}[\rho(\mathbf{x})e^{-\tau x_1 + ik_2 x_2}][\rho(\mathbf{y})e^{-\tau y_1 - ik_2 y_2}], \end{aligned} \qquad \text{(B6)}$$

which is clearly non-negative. This concludes the proof that $|\mathbf{x}|^{-p}$ is reflection positive for all $p > 0$.

APPENDIX C: KAC INTERACTIONS

In this appendix, we add some comments about the possible structure of the GS of Eq. (1) in the case that v is a 2D Kac potential, i.e., $v(\mathbf{x}) = \gamma^2 v_0(\gamma \mathbf{x})$, with γ a small parameter. These may be relevant for the understanding of the "froth problem," addressed by Lebowitz and Penrose in Ref. 59. To be definite and make things simple, we restrict to the case of exponential interactions depending on the Manhattan distance: $v(\mathbf{x}) = \gamma^2 e^{-\gamma \|\mathbf{x}\|_1}$. In this case, $J_c = 2\gamma^{-1}A_\gamma$ and, if $J \geqslant J_c$, the GS is the homogeneous FM state.

From the computations in Sec. III, we already know that, as $J \to J_c^-$, the stripe state is energetically favored as compared to the checkerboard state. If $e_s^*(J) = \min_{h \in \mathbb{N}} e_s(h)$ and $e_c^*(J) = \min_{h \in \mathbb{N}} e_c(h)$ are the optimal stripe and checkerboard energies, an explicit computation shows that, if $0 < \xi := \gamma(J_c - J) \ll 1$,

$$\begin{aligned} e_s^*(J) &= -\frac{2\xi}{|\log \xi|} + O\left(\frac{\xi \log |\log \xi|}{(\log \xi)^2}\right), \\ e_c^*(J) &= -\frac{\xi^2}{2B_\gamma} + O(e^{-1/\xi}); \end{aligned} \qquad \text{(C1)}$$

correspondingly, the scales h_s^* and h_c^* of the optimal stripe and checkerboard configurations turn out to be

$$\begin{aligned} q_c^* &:= \frac{\gamma h_c^*}{2} = \frac{2B_\gamma}{\xi} + O(e^{-1/\xi}), \\ q_s^* &:= \frac{\gamma h_s^*}{2} = \frac{1}{2}|\log \xi| + O(\log |\log \xi|). \end{aligned} \qquad \text{(C2)}$$

Using methods similar to those in the proof of Ref. 1, Theorem 3, it is easy to prove that for ξ small the scaling of $e_s^*(J)$ is the optimal one; i.e., the absolute ground-state energy per site e_0 admits a lower bound of the form $e_0 \geqslant -(\text{const})\xi |\log \xi|^{-1}$.

It is interesting that the model with exponential Kac interactions also displays a phase where mesoscopic checkerboard are energetically favored with respect to stripes. In fact, note that the periods of the optimal checkerboard and striped states are given by

$$\gamma J = \left(2A_\gamma - 2B_\gamma \frac{\tanh q_c^*}{q_c^*}\right)[\tanh q_c^* - q_c^*(1 - \tanh^2 q_c^*)], \quad \text{(C3)}$$

$$\gamma J = 2A_\gamma[\tanh q_s^* - q_s^*(1 - \tanh^2 q_s^*)], \qquad \text{(C4)}$$

from which we immediately recognize that, if $\gamma \ll 1$ and $1 \lesssim J \ll \gamma^{-1}$, then h_c^* and h_s^* are both $\ll \gamma^{-1}$; therefore, the solution to these equations can be determined by expanding their right-hand sides in Taylor series in q and solving to dominant order, which leads to

$$\frac{\gamma h_c^*}{2} = \left(\frac{9\gamma J}{4}\right)^{1/5} + O[(\gamma J)^{3/5}],$$

$$e_c^* = -2 + \frac{10}{9}\left(\frac{9\gamma J}{4}\right)^{4/5} + O[(\gamma J)^{6/5}],$$

$$\frac{\gamma h_s^*}{2} = \left(\frac{3\gamma J}{4}\right)^{1/3} + O(\gamma J),$$

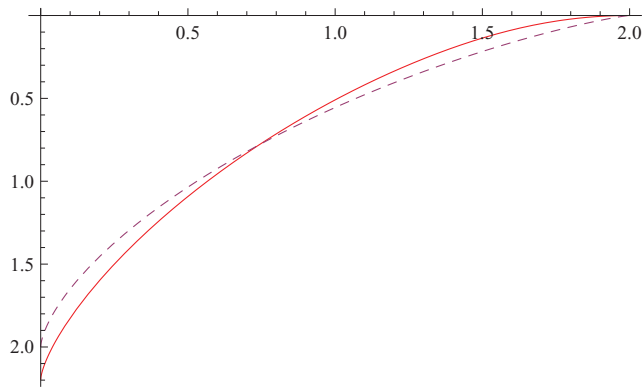$$e_s^* = -2 + 2\left(\frac{3\gamma J}{4}\right)^{2/3} + O[(\gamma J)^{4/3}].$$

FIG. 3. (Color online) A plot of the optimal checkerboard energy e_c^* (solid line) and of the optimal striped energy e_s^* (dashed line) vs $\tilde{J} := \gamma J$ for exponential Kac interactions $v(\mathbf{x}) = \gamma^2 e^{-\gamma\|\mathbf{x}\|_1}$ at $\gamma = 0.4$. The plot shows a transition from a case where $e_c^* < e_s^*$ (for small values of $\tilde{J}$) to a case where $e_c^* > e_s^*$ (for larger values of $\tilde{J}$). In the limit $\gamma \ll 1$, the transition is expected to occur for J of the order γ^{-1}.

Therefore, in this regime, the specific energy e_c^* of the optimal checkerboard configuration is smaller than the specific energy e_s^* of the optimal striped configuration. This suggests that, for any fixed J and γ small enough, the ground states of the considered model display periodic checkerboard order, a conjecture supported by the fact that the absolute ground-state energy per site admits a lower bound of the form $e_0 \geqslant -2 + (\mathrm{const})(\gamma J)^{4/5}$, which has the right scaling (see below for a proof).

In conclusion, if the AF interaction is exponential with a Kac-type scaling, we expect that as J is increased from 0 to J_c, the GS should display a transition from checkerboard to stripes. On the basis of the previous computations, we expect the transition to take place at values of γJ of order one (see Fig. 3).

Remark. The scaling of the checkerboard energy as well as the very existence of a checkerboard phase may depend on the specific choice of the Kac potential. In particular, it may depend on the reflection-positivity property of the Kac potential (note that the considered exponential interaction is reflection positive); if v_0 is smoother at the origin [e.g., $v_0(\mathbf{x}) = e^{-|\mathbf{x}|^2}$], the checkerboard phase may disappear or, at least, be characterized by a completely different scaling behavior. The reason for this is already apparent in a 1D toy model: consider model Eq. (1) in $d = 1$ with $v(x) = \gamma v_0(\gamma x)$ and v_0 either of the form $v_0(x) = e^{-|x|}$ or $v_0(x) = e^{-x^2}$; if one optimizes the energy of a configuration consisting of blocks of uniformly magnetized spins of size h and alternating sign, the optimal size turns out to be of the order $\gamma^{-2/3}$ in the exponential case and $\gamma^{-1}/|\log\gamma|$ in the Gaussian case. This can be seen as follows: The scale of the optimal periodic structure can be found by balancing the energy contributions from the FM and AF interactions; while the first is $2J/h$, the second is of the order of $\hat{v}_0(1/\gamma h)$, with $\hat{v}_0$ the Fourier transform of v_0; the latter depends on the smoothness properties of v_0 and, more specifically, it behaves like $\hat{v}_0(k) \sim k^{-2}$ or $\sim e^{-(\mathrm{const})k^2}$ at large k, in the cases of v_0 exponential or Gaussian, respectively.

Minimization of $2J/h + \hat{v}_0(1/\gamma h)$ over h gives the optimal size of the structures.

The fact that the nature of the checkerboard structure depends on the reflection-positivity properties of the Kac potential is consistent with the fact that the proof of the lower bound on the energy in the Kac regime heavily uses reflection positivity (see next section).

1. Lower bound on the energy: Kac regime

Let us assume that $1 \lesssim J \ll \gamma^{-1}$: In this case, we want to prove that $e_0 \geqslant -2 + (\mathrm{const})(\gamma J)^{4/5}$, which asymptotically matches the upper bound $e_0 \leqslant e_c^*$ and supports the conjecture that, in this regime, the ground state has checkerboard order. Let $E_\Lambda(\underline{\sigma}_\Lambda)$ be the energy of the spin configuration $\underline{\sigma}_\Lambda$ in the periodic squared box Λ. Let us consider a partition of Λ into squares Q_i of side ℓ: $\Lambda = \cup_{i=1}^{|\Lambda|/\ell^2}$; given $\underline{\sigma}_\Lambda$ and Q_i we shall denote by $\underline{\sigma}_{Q_i}$ the restriction of the spin configuration $\underline{\sigma}_\Lambda$ to the square Q_i. Let $v_\gamma^\Lambda(\mathbf{x}) = \gamma^2 \sum_{\mathbf{n}\in\mathbb{Z}^2} e^{-\gamma|\mathbf{x}+\mathbf{n}L|_1}$ and let us rewrite

$$E_\Lambda(\underline{\sigma}_\Lambda) = -2\frac{(\gamma/2)^2}{\tanh^2(\gamma/2)}|\Lambda| + E_\gamma^\Lambda(\underline{\sigma}_\Lambda) + E_J^\Lambda(\underline{\sigma}_\Lambda), \quad \text{(C5)}$$

where $E_\gamma^\Lambda(\underline{\sigma}_\Lambda) = \frac{1}{2}\sum_{\mathbf{x},\mathbf{y}\in\Lambda} v_\gamma^\Lambda(\mathbf{x}-\mathbf{y})\sigma_\mathbf{x}\sigma_\mathbf{y}$ is the antiferromagnetic energy associated to $\underline{\sigma}_\Lambda$, while $E_J^\Lambda(\underline{\sigma}_\Lambda) = 2J\sum_{\mathbf{x}\in\Lambda}\sum_{i=1}^2 \chi(\sigma_\mathbf{x} \neq \sigma_{\mathbf{x}+\hat{e}_i})$ is the surface tension energy of $\underline{\sigma}_\Lambda$ in the box Λ with periodic boundary conditions. If we drop the surface tension energy across the boundaries of the squares Q_i, we get a lower bound on the energy of the form

$$E_\Lambda(\underline{\sigma}_\Lambda) \geqslant -2\frac{(\gamma/2)^2}{\tanh^2(\gamma/2)}|\Lambda| + E_\gamma^\Lambda(\underline{\sigma}_\Lambda) + \sum_{i=1}^{|\Lambda|/\ell^2} \widetilde{E}_J^{Q_i}(\underline{\sigma}_{Q_i}),$$

$$\text{(C6)}$$

where $\widetilde{E}_J^{Q_i}(\underline{\sigma}_{Q_i})$ is the surface tension energy of the spin configuration $\underline{\sigma}_{Q_i}$ in the box Q_i with open boundary conditions. If $m_i := \ell^{-2}\sum_{\mathbf{x}\in Q_i}(\underline{\sigma}_{Q_i})_\mathbf{x}$, the surface tension energy can be further bounded from below by

$$\widetilde{E}_J^{Q_i}(\underline{\sigma}_{Q_i}) \geqslant 2J\ell \min\{1, 2\sqrt{2(1-|m_i|)}\}. \quad \text{(C7)}$$

Moreover, using reflection positivity,[52] the antiferromagnetic energy can be bounded from below as

$$E_\gamma^\Lambda(\underline{\sigma}_\Lambda) \geqslant \ell^2 \sum_{i=1}^{|\Lambda|/\ell^2} e_\gamma(\underline{\sigma}_{Q_i}), \quad \text{(C8)}$$

where $e_\gamma(\underline{\sigma}_{Q_i})$ is the specific energy of the infinite volume configuration obtained by repeatedly reflecting $\underline{\sigma}_{Q_i}$ (with "antiferromagentic reflections") across the sides of Q_i and its images. More explicitly,

$$e_\gamma(\underline{\sigma}_{Q_i}) = \frac{2}{\ell^4} \sum_{\substack{\mathbf{p}=\frac{\pi}{\ell}(n_1,n_2) \\ n_i=1,3,5,\ldots,2\ell-1}} |\tilde{\sigma}_\mathbf{p}|^2 \gamma^2(1-e^{-2\gamma})^2$$

$$\times \prod_{i=1}^2 \frac{1}{(1-e^{-\gamma})^2 + 2e^{-\gamma}(1-\cos p_i)},$$

$$\text{(C9)}$$

where $\widetilde{\sigma}_{\mathbf{p}} := \sum_{\mathbf{x} \in Q_i} \sigma_{\mathbf{x}} e^{-i\mathbf{p}\mathbf{x}}$. Using the fact that, for all $\varepsilon > 0$,

$$|\widetilde{\sigma}_{\mathbf{p}}|^2 \geqslant \frac{4(1-\varepsilon)}{(1-\cos p_1)(1-\cos p_2)} - \frac{1}{\varepsilon}\ell^4(1-|m_i|)^2, \quad \text{(C10)}$$

we get

$$e_{\gamma}(\underline{\sigma}_{Q_i}) \geqslant (1-\varepsilon)e_{\gamma}(\underline{1}_{Q_i}) - (\text{const})\frac{1}{\varepsilon}(1-|m_i|)^2(\gamma\ell)^4, \quad \text{(C11)}$$

where $e_{\gamma}(\underline{1}_{Q_i})$ is the antiferromagnetic energy per site of the checkerboard configuration with tiles of side ℓ. Note that $e_{\gamma}(\underline{1}_{Q_i})$ scales as $(\text{const})(\gamma\ell)^4$ in the regime under consideration and for $\ell \gg 1$; moreover, it can be bounded from below by $\bar{C}(\gamma\ell)^4$ for a suitable constant $\bar{C}$. Optimizing over ε, we get

$$e_{\gamma}(\underline{\sigma}_{Q_i}) \geqslant e_{\gamma}(\underline{1}_{Q_i}) - c(1-|m_i|)(\gamma\ell)^4 \quad \text{(C12)}$$

for a suitable constant c. Combining all the previous bounds, we find that $E_{\Lambda}(\underline{\sigma}_{\Lambda}) + 2(\gamma/2)^2 \tanh^{-2}(\gamma/2)|\Lambda|$ can be bounded from below by

$$\ell^2 \sum_{i=1}^{|\Lambda|/\ell^2} \left\{ \frac{2J}{\ell}\min\{1, 2\sqrt{2(1-|m_i|)}\} \right.$$
$$\left. + [\bar{C} - c(1-|m_i|)](\gamma\ell)^4 \right\}. \quad \text{(C13)}$$

Optimizing over m_i and ℓ leads to $\ell = (\text{const})(J\gamma^{-4})^{1/5}$ and

$$e_0 \geqslant -2\frac{(\gamma/2)^2}{\tanh^2(\gamma/2)}|\Lambda| + (\text{const})(\gamma J)^{4/5} \quad \text{(C14)}$$

as desired. The proof of (C14) can be easily adapted to higher dimensions and to cases where the ferromagnetic interaction has finite range rather than being nearest neighbor. On the contrary, the assumption of RP was used in a crucial way and it is likely that, in the presence of more general long-ranged antiferromagnetic interactions, the ground-state energy scales differently with γ.

[1] A. Giuliani, J. L. Lebowitz, and E. H. Lieb, Phys. Rev. B **74**, 064420 (2006).

[2] A. Giuliani, J. L. Lebowitz, and E. H. Lieb, Phys. Rev. B **76**, 184426 (2007).

[3] A. Giuliani, J. L. Lebowitz, and E. H. Lieb, Commun. Math. Phys. **286**, 163 (2009).

[4] A. Giuliani, J. L. Lebowitz, and E. H. Lieb, Phys. Rev. B **80**, 134420 (2009).

[5] P. Ball, *The Self-Made Tapestry: Pattern Formation in Nature* (Oxford University Press, New York, 2001).

[6] J. Choi, J. Wu, C. Won, Y. Z. Wu, A. Scholl, A. Doran, T. Owens, and Z. Q. Qiu, Phys. Rev. Lett. **98**, 207205 (2007).

[7] K. De'Bell, A. B. Mac Issac, and J. P. Whitehead, Rev. Mod. Phys. **72**, 225 (2000).

[8] V. J. Emery and S. A. Kivelson, Phys. C (Amsterdam) **209**, 597 (1993).

[9] J. Maclennan and M. Seul, Phys. Rev. Lett. **69**, 2082 (1992).

[10] J. A. Robertson, S. A. Kivelson, E. Fradkin, A. C. Fang, and A. Kapitulnik, Phys. Rev. B **74**, 134507 (2006).

[11] N. Saratz, A. Lichtenberger, O. Portmann, U. Ramsperger, A. Vindigni, and D. Pescia, Phys. Rev. Lett. **104**, 077203 (2010).

[12] M. Seul and D. Andelman, Science **267**, 476 (1995).

[13] B. Spivak and S. A. Kivelson, Ann. Phys. (NY) **321**, 2071 (2006).

[14] A. D. Stoycheva and S. J. Singer, Phys. Rev. Lett. **84**, 4657 (2000).

[15] J. Wu, J. Choi, C. Won, Y. Z. Wu, A. Scholl, A. Doran, Chanyong Hwang, and Z. Q. Qiu, Phys. Rev. B **79**, 014429 (2009).

[16] S. Kondo and T. Miura, Science **329**, 1616 (2010).

[17] A. M. Turing, Philos. Trans. R. Soc. London B **237**, 3 (1952).

[18] S. A. Cannas, M. F. Michelon, D. A. Stariolo, and F. A. Tamarit, Phys. Rev. B **73**, 184425 (2006).

[19] S. A. Pighin and S. A. Cannas, Phys. Rev. B **75**, 224433 (2007).

[20] E. Rastelli, S. Regina, and A. Tassi, Phys. Rev. B **73**, 144418 (2006).

[21] R. Czech and J. Villain, J. Phys. Condens. Matter **1**, 619 (1989).

[22] M. Grousson, G. Tarjus, and P. Viot, Phys. Rev. E **62**, 7781 (2000).

[23] U. Löw, V. J. Emery, K. Fabricius, and S. A. Kivelson, Phys. Rev. Lett. **72**, 1918 (1994).

[24] A. B. MacIsaac, J. P. Whitehead, M. C. Robinson, and K. De'Bell, Phys. Rev. B **51**, 16033 (1995).

[25] Z. Nussinov, e-print arXiv:cond-mat/0105253.

[26] P. Politi, Comments Cond. Matter Phys. **18**, 191 (1998).

[27] A. DeSimone, R. V. Kohn, F. Otto, and S. Müller, in *The Science of Hysteresis II: Physical Modeling, Micromagnetics, and Magnetization Dynamics*, edited by G. Bertotti and I. Mayergoyz (Elsevier, New York, 2001), pp. 269–381.

[28] C. B. Muratov, Commun. Math. Phys. **299**, 45 (2010).

[29] Ar. Abanov, V. Kalatsky, V. L. Pokrovsky, and W. M. Saslow, Phys. Rev. B **51**, 1023 (1995).

[30] D. G. Barci and D. A. Stariolo, Phys. Rev. B **79**, 075437 (2009).

[31] S. A. Brazovskii, Zh. Eksp. Teor. Fiz. **68**, 175 (1975) [Sov. Phys. JETP **41**, 85 (1975)].

[32] A. B. Kashuba and V. L. Pokrovsky, Phys. Rev. B **48**, 10335 (1993).

[33] V. J. Emery, E. Fradkin, S. A. Kivelson, and T. C. Lubensky, Phys. Rev. Lett. **85**, 2160 (2000).

[34] J. Lorenzana, C. Castellani, and C. Di Castro, Phys. Rev. B **64**, 235127 (2001); **64**, 235128 (2001).

[35] C. B. Muratov, Phys. Rev. E **66**, 066108 (2002).

[36] C. Ortix, J. Lorenzana, and C. Di Castro, Phys. Rev. Lett. **100**, 246402 (2008).

[37] O. Portmann, A. Golzer, N. Saratz, O. V. Billoni, D. Pescia, and A. Vindigni, Phys. Rev. B **82**, 184409 (2010).

[38] P. C. Hohenberg and J. B. Swift, Phys. Rev. E **52**, 1828 (1995).

[39] Y. Shiwa, J. Stat. Phys. **124**, 1207 (2006).

[40] F. Cinti, O. Portmann, D. Pescia, and A. Vindigni, Phys. Rev. B **79**, 214434 (2009).

[41] G. A. Gehring and M. Keskin, J. Phys. Condens. Matter **5**, L581 (1993).

[42] A. Vindigni, N. Saratz, O. Portmann, D. Pescia, and P. Politi, Phys. Rev. B **77**, 092414 (2008).

[43]B. Kaplan and G. A. Gehring, J. Magn. Magn. Mater. **128**, 111 (1993).

[44]Y. Yafet and E. M. Gyorgy, Phys. Rev. B **38**, 9145 (1988).

[45]T. Garel and S. Doniach, Phys. Rev. B **26**, 325 (1982).

[46]E. Nielsen, R. N. Bhatt, and D. A. Huse, Phys. Rev. B **77**, 054432 (2008).

[47]N. Abu-Libdeh and D. Venus, Phys. Rev. B **80**, 184412 (2009).

[48]N. Abu-Libdeh and D. Venus, Phys. Rev. B **81**, 195416 (2010).

[49]M. Grousson, G. Tarjus, and P. Viot, Phys. Rev. Lett. **86**, 3455 (2001).

[50]O. Osenda, F. A. Tamarit, and S. A. Cannas, Phys. Rev. E **80**, 021114 (2009).

[51]J. Schmalian and P. G. Wolynes, Phys. Rev. Lett. **85**, 836 (2000).

[52]J. Fröhlich, R. Israel, E. H. Lieb, and B. Simon, Commun. Math. Phys. **62**, 1 (1978); J. Stat. Phys. **22**, 297 (1980).

[53]E. Edlund and M. Nilsson Jacobi, Phys. Rev. Lett. **105**, 137203 (2010).

[54]R. Jamei, S. Kivelson, and B. Spivak, Phys. Rev. Lett. **94**, 056805 (2005).

[55]B. Spivak, Phys. Rev. B **67**, 125205 (2003).

[56]B. Spivak and S. A. Kivelson, Phys. Rev. B **70**, 155114 (2004).

[57]E. H. Lieb and M. Loss, *Analysis. Second Edition* (American Mathematical Society, Providence, RI, 2001).

[58]R. Frank and E. H. Lieb, Calc. Variat. Partial Differ. Equations **39**, 85 (2010).

[59]J. L. Lebowitz and O. Penrose, J. Math. Phys. **7**, 98 (1966).